M.Tech (Geotechnical Engineering) Shivakar Sharma (23/GTE/05) 2025

GIS-Based Comparative Analysis of Landslide Susceptibility Using Shannon Entropy, Weight of Evidence, and Information Value: A Case Study of Solan District.

MAJOR I REPORT

A Dissertation Submitted
In Partial Fulfillment of the Requirements for the Degree of

MASTERS OF TECHNOLOGY

IN
GEOTECHNICAL ENGINEERING
BY

Shivakar Sharma
(2K23/GTE/05)

Under the Supervision of

Prof. RAJU SARKAR
Professor
Delhi Technological University

Department of Civil Engineering
DELHI TECHNOLOGICAL UNIVERSITY
(Formerly Delhi College of Engineering)
Shahbad Daulatpur, Main Bawana Road, Delhi-110042

MAY 2025

GIS-Based Comparative Analysis of Landslide Susceptibility Using Shannon Entropy, Weight of Evidence, and Information Value: A Case Study of Solan District.

MAJOR I REPORT

A Dissertation Submitted
In Partial Fulfillment of the Requirements for the Degree of

MASTERS OF TECHNOLOGY

IN
GEOTECHNICAL ENGINEERING
BY

Shivakar Sharma
(2K23/GTE/05)

Under the Supervision of

Prof. RAJU SARKAR
Professor
Delhi Technological University

Department of Civil Engineering
DELHI TECHNOLOGICAL UNIVERSITY
(Formerly Delhi College of Engineering)
Shahbad Daulatpur, Main Bawana Road, Delhi-110042

MAY 2025

DELHI TECHNOLOGICAL UNIVERSITY
(Formerly Delhi College of Engineering)
Shahbad Daulatpur, Main Bawana Road, Delhi-110042

CANDIDATE'S DECLARATION

I, **SHIVAKAR SHARMA,** M. Tech (Geotechnical Engineering) student, having **Roll no: 2K23/GTE/05,** hereby certify that the work which is being presented in the dissertation entitled "**GIS-Based Comparative Analysis of Landslide Susceptibility Using Shannon Entropy, Weight of Evidence, and Information Value: A Case Study of Solan District**" in partial fulfillment of the requirements for the award of the Degree of **Master Of Technology in Geotechnical Engineering**, submitted in the **Department of Civil Engineering, Delhi Technological University**, Delhi Technological University is an authentic record of my work carried out under the supervision of **Prof. Raju Sarkar,** Professor, Department of Civil Engineering, Delhi Technological University, Delhi.

I have not submitted the matter presented in this dissertation for the award of any other degree from this or any other institute.

(SHIVAKAR SHARMA)

This is to certify that the student has incorporated all the corrections suggested by the examiners in the thesis and that the statement made by the candidate is correct to the best of our knowledge.

Prof. RAJU SARKAR
(Supervisor)

Place: Delhi,
Date:

(Signature of Examiner)

DELHI TECHNOLOGICAL UNIVERSITY
(Formerly Delhi College of Engineering)
Shahbad Daulatpur, Main Bawana Road, Delhi-110042

CERTIFICATE BY THE SUPERVISOR(s)

It is certified that **Shivakar Sharma (**2K23/GTE/05) has carried out their research work presented in this report entitled "**GIS-Based Comparative Analysis of Landslide Susceptibility Using Shannon Entropy, Weight of Evidence, and Information Value: A Case Study of Solan District**.**"** for the award of **Master of Technology** from Department of Civil Engineering, Delhi Technological University, Delhi, under my supervision. The report embodies results of original work, and studies are carried out by the student herself and the contents of the report do not form the basis for the award of any other degree to the candidate or to anybody else from this or any other University/Institution.

Prof. RAJU SARKAR
(Supervisor)
Professor
Delhi Technological University

Place: Delhi

Date:

ABSTRACT

Landslide Susceptibility Assessment (LSA) is crucial for understanding and mitigating landslide risks, especially in vulnerable regions like Solan District, Himachal Pradesh, where complex topography, diverse geological formations, and significant precipitation contribute to instability. This study integrates geospatial analysis with statistical modelling techniques to evaluate the influence of various landslide conditioning factors (LCFs), including slope, elevation, aspect, and lithology, on landslide occurrence. Using a landslide inventory of 845 recorded events and GIS-derived thematic layers were used to apply three statistical models: Information Value (IV), Shannon Entropy (SE), and Weight of Evidence (WoE). Among them, the Information Value (IV) model demonstrated the highest predictive accuracy (AUC = 0.737), followed by Shannon Entropy (SE) (AUC = 0.719), while Weight of Evidence (WoE) showed the lowest performance (AUC = 0.632), suggesting limited capability in capturing complex spatial relationships. The resulting susceptibility map categorizes the district into distinct risk zones, aiding in hazard mitigation and land-use planning. Model validation through AUC-ROC analysis and success prediction rate curves confirmed the reliability and predictive accuracy of the applied techniques. This comparative study helps in underscores the importance of combining statistical models with geospatial tools for disaster risk management and infrastructure planning in Solan district.

ACKNOWLEDGEMENT

I, **SHIVAKAR SHARMA**, would like to express my deepest gratitude to all those who have given unforgettable contributions to the successful contribution of this thesis.

I want to thank Prof. Prateek Sharma, Vice Chancellor, for providing all the facilities and helping carry out this project. I thank **Prof. Raju Sarkar**, Associate Dean, for the stimulus provided.

I am extremely grateful to **Dr. K. C. Tiwari**, Professor and Head of the Department of Civil Engineering, for the encouragement and support provided during the project work.

I sincerely thank the coordinator, **Dr. Ashok Kumar Gupta**, Professor, for his valuable suggestions for improvement during project reviews.

I acknowledge with deep gratitude the valuable guidance, encouragement, and suggestions from my project guide, **Prof. Raju Sarkar**, Professor, who has been a constant source of inspiration throughout this project.

I would also like to take this opportunity to thank all the faculty members and non-teaching staff members in the Department of Civil Engineering for their direct and indirect help rendered during the course of the project work.

I want to give a massive token of gratitude to my parents and all family members for their unwavering support and understanding throughout this journey. Their encouragement, motivation, and belief in my abilities have been a constant source of strength.

Lastly, I would like to express my immense gratitude towards god. I wouldn't have been what I am today without his/her blessing. Please, god, always keep me on the list of your much-loved children.

SHIVAKAR SHARMA

2K23/GTE/05

DTU DELHI 110042

TABLE OF CONTENTS

LIST OF TABLES

LIST OF FIGURES

CHAPTER 1

INTRODUCTION

The Solan district of Himachal Pradesh, situated in the southern part of the state, is highly prone to landslides and slope failures due to its intricate topography, varied geological structure, and substantial rainfall. Covering an area of approximately 1,936 square kilometers, the district lies within the Shivalik Hills of the outer Himalayas, with altitudes ranging from 300 to 3,000 meters above sea level. The combination of steep slopes, rugged terrain, and intense monsoon rainfall often leads to soil erosion, rockfalls, and large-scale slope instability. These hazards pose significant threats to human life, infrastructure, and economic stability, highlighting the need for systematic landslide susceptibility assessment.

As one of India's most landslide-prone states, Himachal Pradesh faces increasing vulnerability due to both natural conditions and human interventions, such as deforestation, unregulated development, and road construction. In Solan, these challenges directly impact agriculture, tourism, and infrastructure, making the identification of landslide-prone zones essential for risk reduction and sustainable development. Landslide susceptibility mapping (LSM) offers crucial data to inform disaster management strategies and land-use planning.

The advent of geospatial technologies like Geographic Information Systems (GIS) and Remote Sensing (RS) has revolutionized landslide assessment. These tools, combined with statistical and machine learning techniques, enable efficient analysis of spatial data and accurate susceptibility mapping. This study applies three statistical models—Shannon Entropy, Weight of Evidence (WoE), and Information Value (IV)—to evaluate landslide susceptibility in Solan. These models assign weights to various conditioning factors and determine their relative contributions to slope instability. Key conditioning factors used include slope, aspect, curvature, elevation, lithology, roughness, hillshade, distance to streams, and the topographic wetness index (TWI). Each factor was categorized based on

its influence on landslide occurrence, and corresponding weight values were computed to generate comprehensive susceptibility maps. The Solan landslide inventory, comprising 845 recorded events sourced from NASA's Landslide Catalog and Bhukosh (GSI), was validated using satellite imagery and field observations. The inventory formed the foundation for model training and testing. For spatial analysis, conditioning factors were classified into appropriate intervals—such as slope steepness or lithological stability—and assigned weighted values reflecting their landslide potential. These weights were normalized in entropy-based models and directly used in IV and WoE methods to produce susceptibility outputs. Model accuracy was evaluated using Area Under the Receiver Operating Characteristic Curve (AUC-ROC), through both success and prediction rate curves.

The findings of this study provide practical insights for disaster mitigation and infrastructure development. High-risk zones identified in the susceptibility maps can guide slope stabilization, afforestation, and early warning system implementation. Overall, this research demonstrates the value of integrating geospatial tools with statistical modeling to assess landslide risk. It offers a robust methodological framework for understanding regional vulnerability and enhancing preparedness and sustainable planning in Solan district.

CHAPTER 2

LITERATURE REVIEW

Kincal, C., & Kaycan, H. (2022). Investigates the preparation of a landslide susceptibility map in Izmir, Turkey, using four models: Logistic Regression (LR), Analytical Hierarchy Process (AHP), Frequency Ratio (FR), and Index of Entropy (IOE). The Combined Method (CM) achieved the highest accuracy with an AUC of 0.887, outperforming IOE (AUC = 0.841), AHP (AUC = 0.816), FR (AUC = 0.738), and LR (AUC = 0.727). The study identifies urban residential areas as more landslide-prone compared to rural areas

Pattanaik, A., Singh, T. K., Saxena, M., & Prusty, B. G. (2019). Conducts a landslide susceptibility mapping study in the Mechuka Valley, Arunachal Pradesh, India, using the Analytical Hierarchy Process (AHP). Remote sensing and GIS techniques were utilized to analyze terrain factors such as elevation, slope, lineaments, drainage, land use, and wetness index. These factors were categorized, rated, and weighted to assess their impact on landslides, culminating in the creation of a Landslide Hazard Zonation (LHZ) map for the region.

Lestari, S. F., & Suratman. (2022). Explores landslide susceptibility zones in Nagari Tanjung Sani and Nagari Sungai Batang, West Sumatra, using the Weight of Evidence (WOE) method. Nagari Sungai Batang exhibited translational and rotational landslides with moderate activity and risk, while Nagari Tanjung Sani showed rockfall and topple landslides with high activity and the highest risk. Statistical analysis was applied to identify and assess the susceptibility levels across both areas

Askoy, H. (2023). Investigates the determination of landslide susceptibility using the Analytical Hierarchy Process (AHP) and examines the role of forest ecosystem services on landslide susceptibility. A landslide susceptibility map was developed and evaluated

using the ROC curve method, achieving an AUC value of 0.809. The study analyzed the influence of forest type, stand structure, development stage, crown closure, and stand age on landslide risk by overlaying forest type maps with the landslide susceptibility map using GIS techniques

Miller, S., & Degg, M. (2012). Conducts landslide susceptibility mapping in North-East Wales, producing a comprehensive landslide inventory with 430 identified landslides. Using GIS tools and a multiple logistic regression approach, susceptibility models were developed. The study reveals that 8% of drift deposits and 12% of solid geology areas exhibit high or very high slope instability risk.

Talaab, K., Cheng, T., & Zhang, Y. (2018). Applies the Random Forest algorithm to map landslide susceptibility and classify landslide types in Piedmont, Italy. The study produced highly accurate susceptibility and classification maps, achieving over 85% accuracy. The results demonstrate the effectiveness of the Random Forest algorithm for mapping landslide risks in large and diverse areas, providing detailed and user-friendly outputs.

Orhan, O., Bilgilioglu, S. S., Kaya, Z., Ozcan, A. K., & Bilgilioglu, H. (2022). Assesses and maps landslide susceptibility using five machine learning methods: Artificial Neural Network (ANN), Logistic Regression (LR), Support Vector Machine (SVM), Random Forest (RF), and Classification and Regression Tree (CART). A landslide inventory of 252 events was created, and 11 influencing factors were analyzed. The models were trained, their performances compared, and validated using metrics such as ROC, sensitivity, specificity, F-measure, accuracy, and the kappa index.

Saha, S., Saha, A., Roy, B., Chaudhary, A., & Sarkar, R. (2024). Utilizes an Artificial Neural Network (ANN) and General Linear Model (GLM) ensemble approach to model landslide susceptibility in the Mirik region of West Bengal, India. A dataset of 373

landslide locations and 12 conditioning factors (LCFs) was analyzed, with multicollinearity tests ensuring the selection of suitable LCFs. The ensemble machine learning method was used to develop detailed and accurate landslide susceptibility maps (LSMs) for the region.

Oliveira, S. C., Zêzere, J. L., Garcia, R. A. C., Pereira, S., Vaz, T., & Melo, R. (2024). Investigates uncertainties in rainfall-triggered, event-based landslide inventories for susceptibility assessment in a study area north of Lisbon, Portugal. The study uses two rainfall event-based inventories and a historical inventory to analyze representativeness, reliability, and validation appropriateness. Key findings reveal: (i) similar landslide types may occur under differing rainfall conditions but vary in size and predisposing factors like lithology and soil type; (ii) event-based susceptibility models are unreliable in this region; and (iii) incomplete and non-independent inventories introduce significant uncertainties. The research informs regional landslide susceptibility, early warning system design, and civil protection preparedness.

Chen, S., Wu, L., & Miao, Z. (2022). Examines regional seismic landslide susceptibility by incorporating rock mass strength heterogeneity into permanent-displacement analysis. Traditional methods assign constant strength values per lithology, overlooking spatial heterogeneity and reducing reliability. This study develops an empirical model using a seismic landslide inventory and lithological data to quantify rock mass strength heterogeneity. Incorporating this heterogeneity into susceptibility assessments significantly improves reliability, as demonstrated in two case studies. The findings are crucial for enhancing earthquake emergency response and post-earthquake land use planning.

Badvath, N., Sahoo, S., & Samal, R. (2024). Conducts landslide susceptibility mapping for the West-Jaintia Hills district, Meghalaya, by analyzing various causative factors such as rainfall, slope, geomorphology, elevation, lineament density, LULC, distance from

roads, NDWI, MSAVI, and NDVI. Historical landslide data were divided into training (75%) and testing (25%) samples to assess prediction efficiency. The study provides insights for better landslide risk management and mitigation in the region.

CHAPTER 3
METHODOLOGY

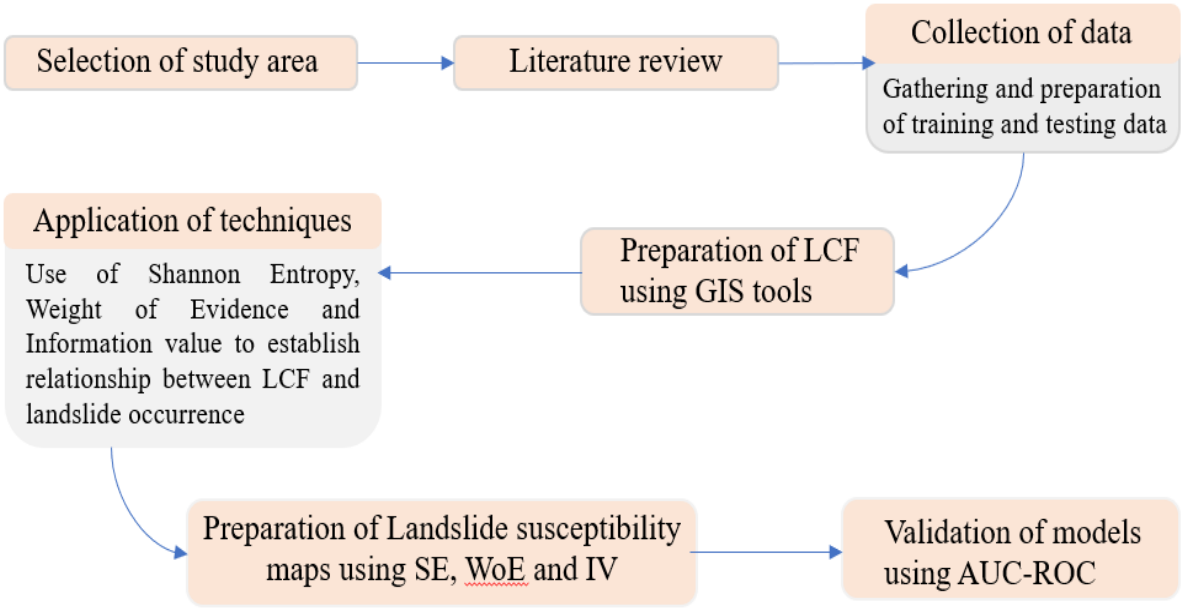

Figure 3.1 Methodology

CHAPTER 4
DATA SOURCE

TABLE 4.1 DATA SOURCE

MAP	DATA SOURCE
INDIAN MAP	https://onlinemaps.surveyofindia.gov.in/Digital_Product_Show.aspx
LANDSLIDE INVENTORY POINTS	https://bhukosh.gsi.gov.in/Bhukosh/Public https://svs.gsfc.nasa.gov/4710
DISTRICT AND SUB-DISTRICT MAPS	https://esriindia1.maps.arcgis.com/home/item.html?id=b89de19cafb94ea38552a55eb5b2d13d
DIGITAL ELEVATION MODEL	https://portal.opentopography.org/datasets
DISTANCE FROM DRAINAGE	https://www.hydrosheds.org/products/hydrorivers#downloads
LITHOLOGY	https://certmapper.cr.usgs.gov/data/apps/world-maps/

CHAPTER 5

STUDY AREA: SOLAN, HIMACHAL PRADESH

Solan district is located in the southern part of Himachal Pradesh, India, and spans an area of approximately 1,936 square kilometers. Geographically, it lies between latitudes 30.05° N to 31.15° N and longitudes 76.42° E to 77.20° E. The district is situated within the Shivalik Hills, a subrange of the outer Himalayas, and exhibits a highly variable terrain with elevations ranging from 300 to 3,000 meters above sea level. Solan's topography includes steep slopes, rugged hills, and narrow valleys, contributing to its complex and dynamic landscape.

The western and southern parts of the district—particularly the Nalagarh and Arki tehsils—are characterized by relatively low-lying terrain, while the central and northeastern areas, including Solan, Kasauli, and Kandaghat tehsils, feature higher altitudes and steeper gradients. The district experiences a sub-tropical to temperate climate, with heavy monsoonal rainfall during July to September, which often triggers soil erosion and slope instability. Rich in natural vegetation and biodiversity, the region is also marked by expanding urban and rural settlements. Due to its geomorphological diversity and climatic conditions, Solan district presents a significant area of interest for environmental and geospatial studies related to slope dynamics and terrain analysis.

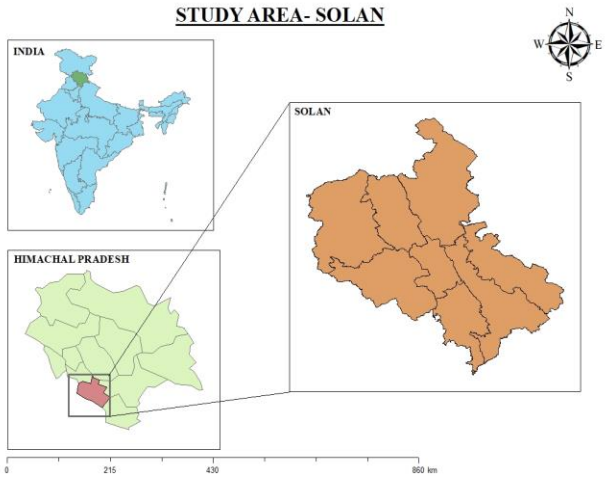

Figure 5.1 Study area

CHAPTER-6

LANDSLIDE INVENTORY MAPS

A Landslide Inventory Map (LIM) records past landslide events along with relevant topographical, geological, and meteorological details. It plays a crucial role in identifying the relationship between landslide occurrences and conditioning factors (CFs), aiding in susceptibility mapping and prediction.

In this study, landslide data in polygon format were obtained from the Bhukosh portal and the NASA Landslide Catalog, both recognized for their authoritative national and global records. A total of 845 landslide points was extracted for the Solan district.

Following common research practices, 70% of the data was used for model training and 30% for testing. These inventory points form the foundation of landslide susceptibility models by linking historical landslide events to environmental variables, enabling accurate identification of high-risk zones.

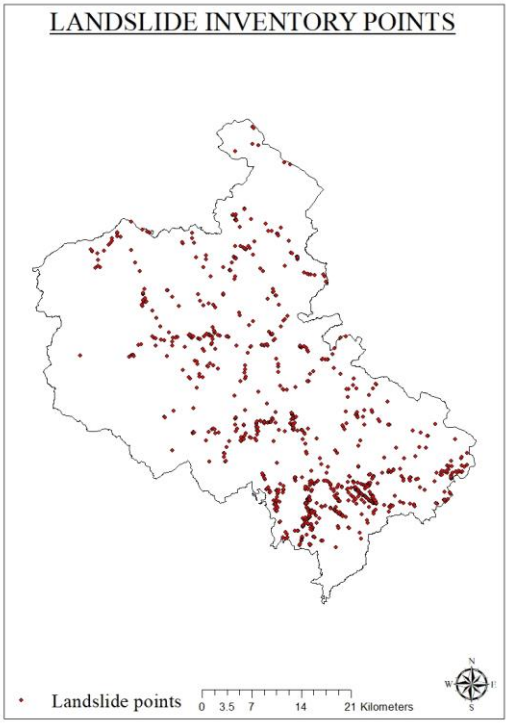

Figure 6.1 Landslide Inventory Points

CHAPTER 7

LANDSLIDE CONDITIONING FACTORS (LCF)

7.1 SLOPE:

Slope, a critical landslide conditioning factor (LCF), represents the steepness or inclination of a surface and plays a significant role in determining slope stability. Steeper slopes are generally more prone to landslides due to the increased gravitational force acting on the surface materials. In the context of Solan district, the slope map was derived from Digital Elevation Model (DEM) data using the spatial analyst tool in ArcGIS. The map was classified into five distinct slope categories, facilitating a detailed analysis of how varying degrees of slope contribute to landslide susceptibility. Understanding slope variations is crucial, as it helps identify areas with a higher likelihood of slope failure, thereby aiding in effective landslide risk assessment and management.

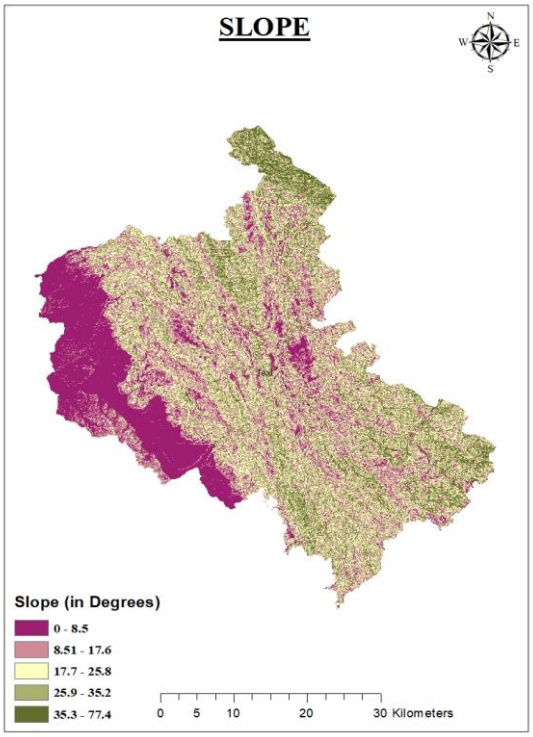

Figure 7.1 SLOPE

7.2 ASPECT:

Aspect, an essential Landslide Conditioning Factor (LCF), refers to the direction a slope faces, typically measured in relation to the cardinal directions. It significantly influences environmental conditions such as sunlight exposure, wind patterns, and moisture retention, all of which affect slope stability. In the study of Solan district, the aspect map was generated using Digital Elevation Model (DEM) data and processed through ArcGIS. Variations in aspect can impact the susceptibility of slopes to landslides, as certain orientations may retain more moisture or be exposed to climatic factors that weaken the terrain. This analysis helps in identifying areas more vulnerable to landslides based on their slope orientation, contributing to more accurate susceptibility mapping and disaster management strategies.

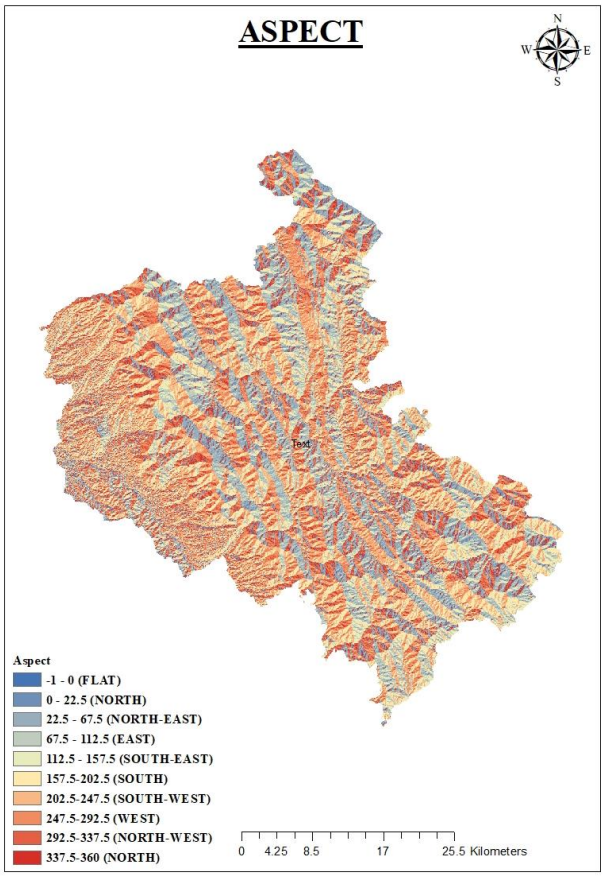

Figure 7.2 ASPECT

7.3 ROUGHNESS:

Roughness, an important Landslide Conditioning Factor (LCF), refers to the irregularity or unevenness of the terrain surface, influencing slope stability and the likelihood of landslides. It plays a crucial role in determining water retention, soil movement, and the mechanical stability of slopes. Areas with higher surface roughness often indicate uneven terrain, which can lead to concentrated runoff, reduced vegetation stability, and an increased likelihood of rock fractures, all of which heighten landslide risk. In the case of Solan district, roughness was calculated using Digital Elevation Model (DEM) data within ArcGIS. Analyzing roughness helps identify areas more susceptible to slope failure, contributing significantly to the creation of accurate landslide susceptibility maps and the development of effective mitigation strategies.

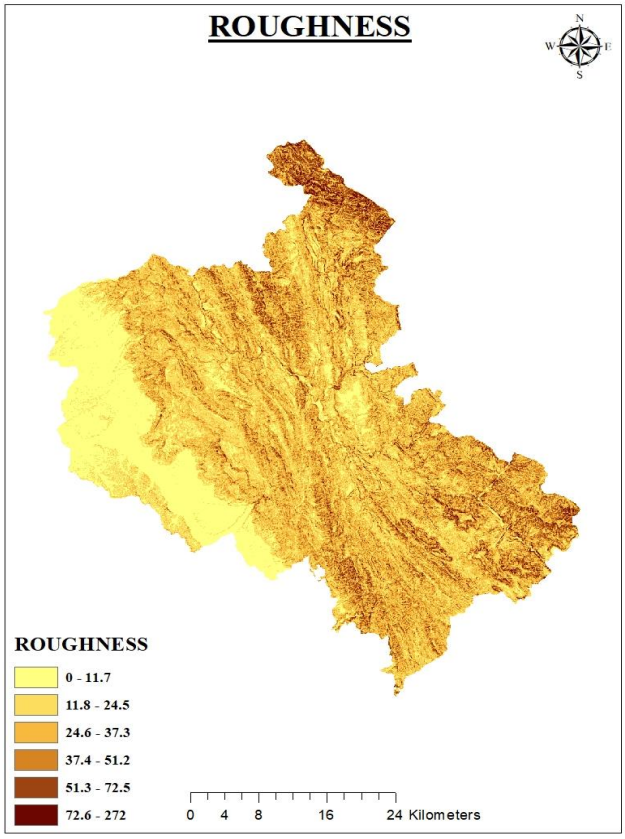

Figure 7.3 ROUGHNESS

7.4 DISTANCE TO STREAM:

Distance to stream is a key Landslide Conditioning Factor (LCF) that measures the horizontal distance from a point on a slope to the nearest drainage channel or water body. This factor significantly influences slope stability, as proximity to streams can increase the risk of undercutting, erosion, and heightened moisture content in the slope material. In regions like Solan district, which experience substantial rainfall, high-velocity discharge and bank erosion near streams exacerbate the potential for slope failure. The distance-to-stream map for the study area was generated using the hydrology tool in ArcGIS. Understanding this factor is crucial for landslide susceptibility mapping, as it highlights the interplay between hydrological processes and terrain instability, thereby aiding in the identification of high-risk zones and effective disaster management planning.

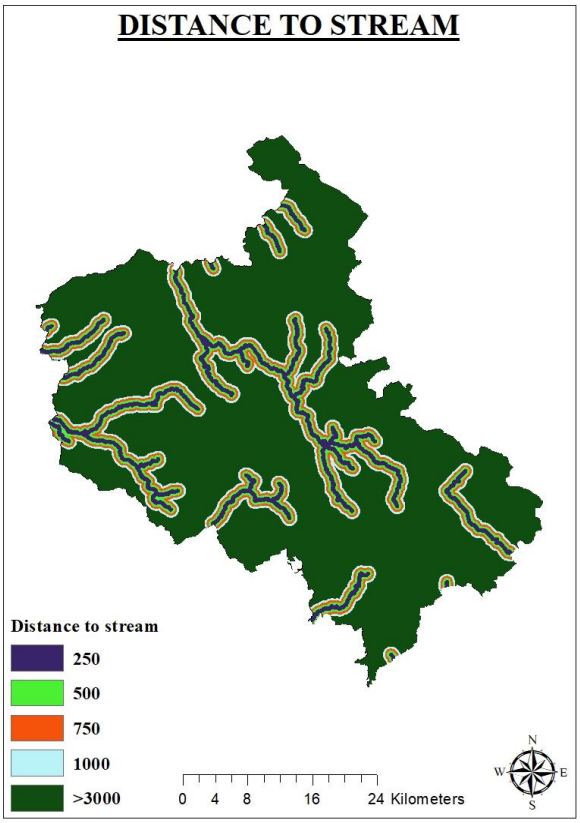

Figure 7.4 DISTANCE TO STREAM

7.5 CURVATURE:

Curvature is a vital Landslide Conditioning Factor (LCF) that reflects the shape of the terrain and its influence on water flow and soil movement. It is derived from Digital Elevation Model (DEM) data and categorized into concave, convex, and planar surfaces. Concave areas tend to collect water, increasing soil saturation and the risk of slope failure, while convex areas promote water flow away, reducing the chances of accumulation. In the context of Solan district, curvature was analyzed using the curvature function in ArcGIS, providing insights into how terrain morphology affects landslide susceptibility. This factor helps identify zones prone to water concentration or erosion, contributing to a more accurate assessment of landslide risk and better planning of mitigation measures.

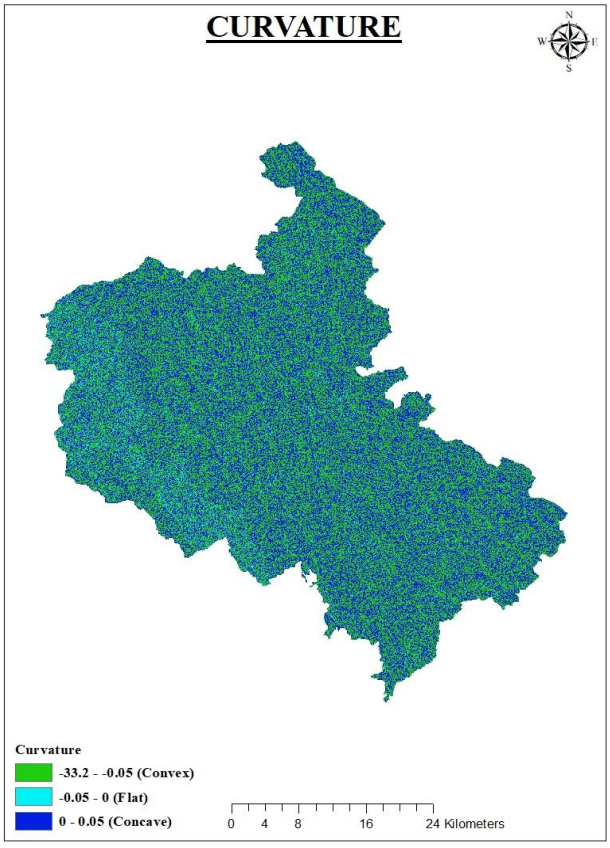

Figure 7.5 CURVATURE

7.6 ELEVATION:

Elevation is a fundamental Landslide Conditioning Factor (LCF) that significantly influences terrain stability and susceptibility to landslides. It impacts various environmental and geological processes, including slope steepness, vegetation distribution, weathering rates, and water flow patterns. Higher elevations are often associated with steeper slopes and greater erosion risks, making them more prone to landslides, while lower elevations may experience debris accumulation and increased water retention, which can also trigger slope failure. In Solan district, elevation varies widely, ranging from 300 to 3,000 meters above sea level. This variation was analyzed using Digital Elevation Model (DEM) data, aiding in the identification of areas with varying landslide susceptibility. Understanding elevation patterns is critical for accurate landslide mapping and implementing effective risk mitigation strategies.

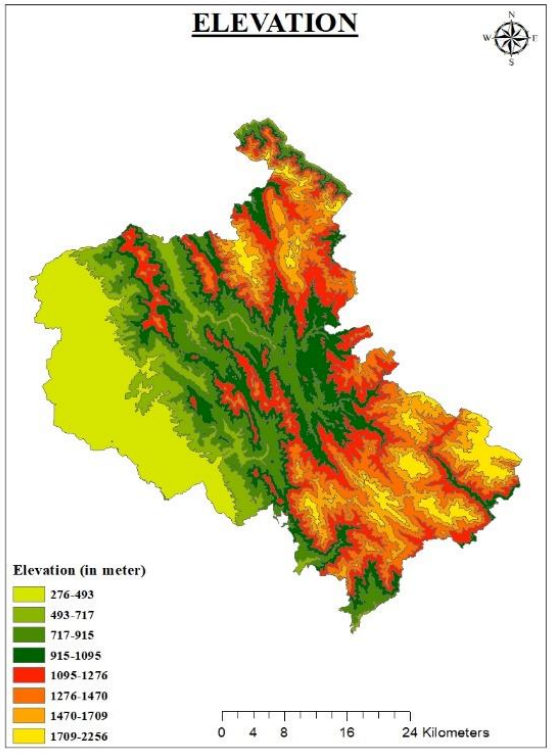

Figure 7. 6 ELEVATION

7.7 HILLSHADE:

Hillshade is an important Landslide Conditioning Factor (LCF) that simulates how sunlight interacts with the terrain, highlighting the landscape's features by representing variations in light and shadow. It provides a detailed visualization of slope orientation and gradient, which are critical in understanding terrain stability. Shaded areas often retain more moisture, leading to higher soil saturation and a potential decrease in slope stability, while sunlit areas are generally drier, reducing landslide risk. In the study of Solan district, hillshade analysis was performed using Digital Elevation Model (DEM) data in ArcGIS, helping to identify zones with varying moisture retention and exposure. By incorporating hillshade into landslide susceptibility mapping, researchers can better understand the interplay between solar radiation, moisture distribution, and slope stability, contributing to more accurate risk assessments.

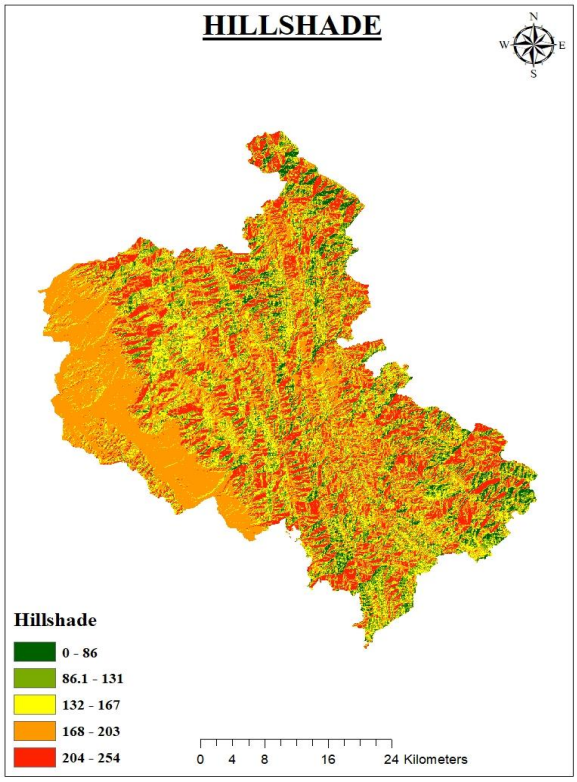

Figure 7 HILLSHADE

7.8 LITHOLOGY:

The India shapefile, sourced from the USGS, initially contained various rock types across the region. Upon further analysis and clipping to focus on the Solan district, five distinct rock types were identified. Each of these rock types has unique characteristics such as composition, strength parameters, and plasticity, which are crucial for understanding their stability. Lithology, which refers to the type and physical properties of rocks and soils in a given area, plays a significant role in landslide susceptibility. Harder rocks generally offer more stability, reducing the likelihood of landslides, whereas softer, more erodible rocks and clay-rich soils are more susceptible to failure due to their weaker structural integrity and higher vulnerability to erosion. These variations in lithology are essential in assessing and mapping landslide risks in the region.

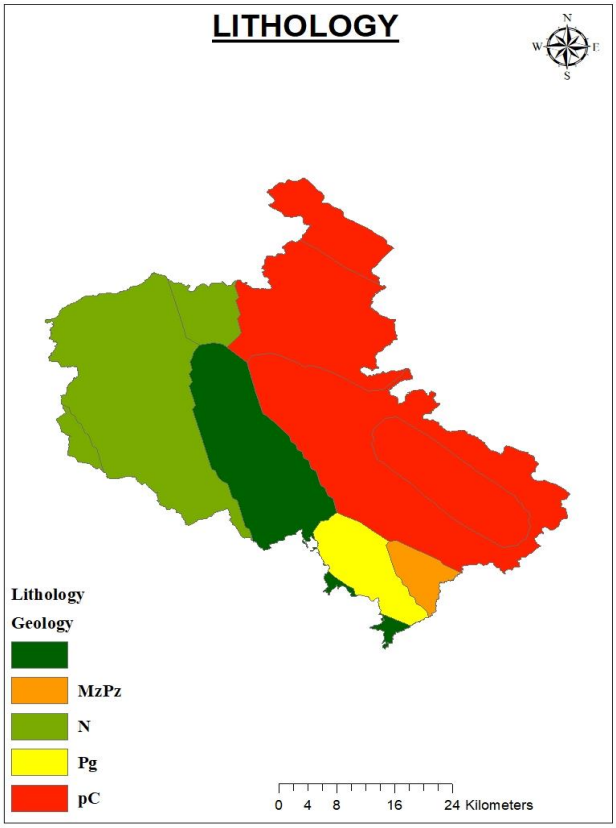

Figure 7.8 LITHOLOGY

7.9 TOPOGRAPHIC WETNESS INDEX (TWI):

The Topographic Wetness Index (TWI) is a spatial index used to assess the relative wetness of a landscape by analyzing its topographic features, particularly the accumulation of water within an area. It is derived by combining several topographic factors, including elevation, slope, and contributing area (or drainage area), to determine how water flows and collects across the terrain. Areas with higher TWI values are typically more prone to water saturation, as they have a greater tendency to accumulate moisture due to their topography, which increases the potential for landslides. On the other hand, regions with lower TWI values are better drained, indicating less water accumulation and a reduced likelihood of saturation-induced landslide risks. TWI is a valuable tool in understanding and mapping the vulnerability of landscapes to landslides and other water-related hazards.

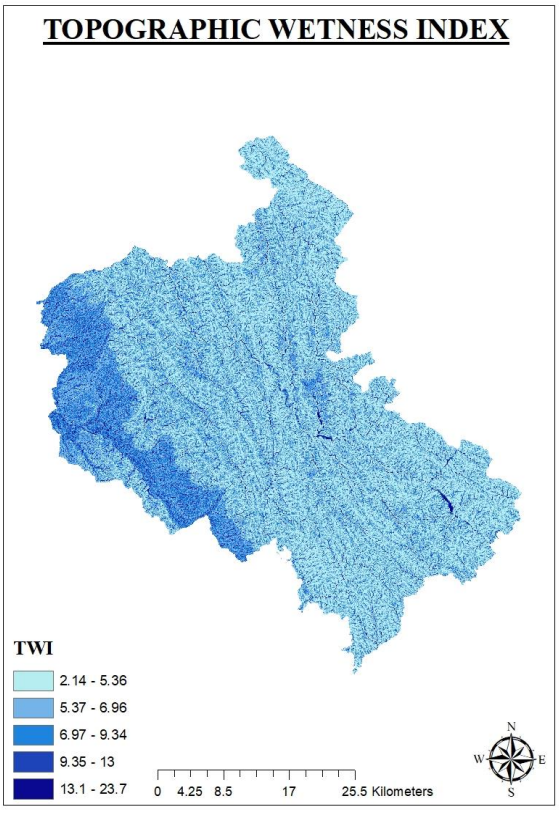

Figure 7.9 TOPOGRAPHIC WETNESS INDEX

CHAPTER-8

SHANNON ENTROPY

8.1 Introduction:

Shannon Entropy is a fundamental concept in information theory that measures the uncertainty or randomness in a system. It quantifies the amount of information required to describe a random variable, serving as a key tool for understanding the unpredictability of a system. In the context of spatial analysis and landslide susceptibility mapping (LSM), Shannon Entropy is applied to evaluate the relative contribution of various factors—such as slope, elevation, and lithology—to the occurrence of landslides. By calculating the entropy of these factors, it helps to assess how much each variable influences the spatial distribution of landslides, enabling more accurate and reliable predictions of landslide-prone areas. This approach aids in reducing uncertainty and improving the understanding of landslide risks.

8.2 Formula:

$$\%FR\ P_{ij} = \frac{\%\ Landslide\ pixels}{\%\ Class\ pixels} \qquad 8.1$$

Where P_{ij} from equation 8.1 represents frequency ratio and (P_{ij}) from equation 8.2 gives probability density value of each class

$$(P_{ij}) = \frac{(P_{ij})}{(\sum_1^n P_{ij})} \qquad 8.2$$

E_{ij} and E_{ijmax} from equation 8.3 and 8.4 denote the entropy values for each class whereas n_{ij} is the number of classes in each factor.

$$E_{ij} = \sum_{i=1}^{n_j} (P_{ij}) * \log(P_{ij}) \qquad 9.3$$

$$E_{ijmax} = \log_2(n_{ij}) \quad 9.4$$

The information coefficient, I_j, and the final weight index, W_j were evaluated using equations 8.5 and 8.6 respectively.

$$I_{ij} = \frac{H_{jmax} - H_j}{H_{jmax}} \quad 8.5$$

$$W_j = I_J \times P_j \quad 8.6$$

8.3 Outcome:

The outcome of using Shannon Entropy in landslide susceptibility mapping is the generation of normalized entropy values, which act as weights to quantify the influence of each landscape classification factor (LCF) on landslide susceptibility. These normalized entropy values indicate how strongly each factor, such as slope, aspect, or curvature, contributes to the likelihood of landslides occurring in a given area. By combining these weights with the different LCFs, a more refined and accurate landslide susceptibility map is created. This map highlights regions with varying levels of risk, offering a valuable tool for assessing areas that are more prone to landslides and assisting in risk management and mitigation strategies.

8.4 Advantage:

Shannon Entropy offers several advantages when used in landslide susceptibility mapping (LSM). It provides an objective and data-driven approach to quantify the influence of each landslide conditioning factor, reducing subjectivity in the weighting process. The method is particularly effective in handling uncertainty and variability within spatial datasets, making it suitable for complex terrains like the Solan district. It also integrates well with GIS platforms, allowing for efficient spatial analysis and map generation. Additionally, Shannon Entropy can be applied even in areas with limited

ground truth data, as it relies on the statistical relationships between landslide occurrences and environmental factors. By generating normalized weights, it enhances the accuracy and reliability of susceptibility maps, supporting better risk assessment and management strategies.

.

8.5 Application:

Shannon Entropy is applied in landslide susceptibility mapping by combining a landslide inventory with various landslide conditioning factors (LCFs), such as slope, elevation, aspect, and lithology. The landslide inventory provides historical data of landslide occurrences, while the conditioning factors represent the environmental and topographical variables that influence landslide risks. By integrating these elements, Shannon Entropy helps quantify the uncertainty and relative importance of each factor in determining landslide susceptibility in a given study area. Beyond landslides, this approach is also used for assessing other natural hazards such as floods, soil erosion, and other environmental risks. In these applications, Shannon Entropy aids in creating risk maps that highlight areas vulnerable to such hazards, supporting effective disaster management and mitigation planning.

8.6 Data table:

Table 8.1 SHANNON ENTROPY CALCULATION

Data Layer	Classes	Class pixels	Landslide pixels	% Class pixels	% Landslide pixels	FR	FR(%)	Pij	Eij	1-Eij	Wj
SLOPE (in Degrees)											
0-6.98	1	372274	6	0.186	0.007	0.000016	0.040	0.005	-0.011		
6.98-14	2	338188	44	0.169	0.055	0.000130	0.323	0.037	-0.053		
14-20.3	3	409173	142	0.205	0.176	0.000347	0.861	0.098	-0.099		
20.3-26.4	4	385657	217	0.193	0.269	0.000563	1.396	0.159	-0.127		

26.4-32.8	**5**	**280540**	**191**	**0.140**	**0.237**	**0.000681**	**1.689**	**0.192**	**-0.138**		
32.8-41	**6**	**161733**	**166**	**0.081**	**0.206**	**0.001026**	**2.546**	**0.290**	**-0.156**		
41-77.4	**7**	**51448**	**40**	**0.026**	**0.050**	**0.000777**	**1.928**	**0.220**	**-0.145**		
TOTAL		**1999013**	**806**			**0.003541**	**8.781**	**1**	**0.727**	**0.273**	**0.082**
ASPECT											
-1 (Flat)	**1**	**11282**	**2**	**0.005**	**0.002**	**0.000177**	**0.470**	**0.190**	**-0.137**		
0-22.5 (North)	**2**	**116611**	**40**	**0.054**	**0.050**	**0.000343**	**0.910**	**0.368**	**-0.160**		
22.5-67.5 (North-east)	**3**	**261477**	**107**	**0.122**	**0.133**	**0.000409**	**1.086**	**0.439**	**-0.157**		
67.5-112.5 (East)	**4**	**246419**	**87**	**0.115**	**0.108**	**0.000353**	**0.001**	**0.001**	**-0.002**		
112.5-157.5 (South-east)	**5**	**218320**	**77**	**0.102**	**0.095**	**0.000353**	**0.001**	**0.001**	**-0.002**		
157.5-202.5 (South)	**6**	**279443**	**102**	**0.131**	**0.126**	**0.000365**	**0.001**	**0.001**	**-0.002**		
202.5-247.5 (South-west)	**7**	**339281**	**157**	**0.158**	**0.195**	**0.000463**	**0.001**	**0.000**	**-0.001**		
247.5-292.5 (West)	**8**	**310660**	**122**	**0.145**	**0.151**	**0.000393**	**0.001**	**0.000**	**-0.002**		
292.5-337.5 (North-west)	**9**	**246277**	**78**	**0.115**	**0.097**	**0.000317**	**0.001**	**0.001**	**-0.002**		
337.5-360 (North)	**10**	**111116**	**35**	**0.052**	**0.043**	**0.000315**	**0.001**	**0.001**	**-0.002**		
TOTAL		**2140886**	**807**				**2.475**		**0.466**	**0.534**	**0.161**
ROUGHNESS											
0-11.7	**1**	**425176**	**8**	**0.198**	**0.010**	**0.000019**	**0.050**	**0.006**	**-0.014**		
11.7-24.5	**2**	**585018**	**107**	**0.272**	**0.132**	**0.000183**	**0.485**	**0.063**	**-0.075**		
24.5-36.3	**3**	**596507**	**283**	**0.277**	**0.349**	**0.000474**	**1.258**	**0.162**	**-0.128**		
36.3-50.1	**4**	**377922**	**260**	**0.176**	**0.321**	**0.000688**	**1.825**	**0.235**	**-0.148**		
50.1-71.5	**5**	**143994**	**140**	**0.067**	**0.173**	**0.000972**	**2.579**	**0.333**	**-0.159**		
71.5-272	**6**	**22205**	**13**	**0.010**	**0.016**	**0.000585**	**1.553**	**0.200**	**-0.140**		
TOTAL		**2150822**	**811**				**7.749**		**0.664**	**0.336**	**0.101**
HILLSHADE											
0-86	**1**	**114543**	**100**	**0.054**	**0.125**	**0.000873**	**2.323**	**0.363**	**-0.160**		
86-131	**2**	**312874**	**156**	**0.146**	**0.194**	**0.000499**	**1.327**	**0.208**	**-0.142**		

131-167	3	457373	163	0.214	0.203	0.000356	0.948	0.148	-0.123		
167-203	4	797037	180	0.373	0.224	0.000226	0.601	0.094	-0.097		
203-254	5	455090	204	0.213	0.254	0.000448	1.193	0.187	-0.136		
TOTAL		2136917	803				6.392		0.657	0.343	0.103
CURVATURE											
-33.2- (-0.05)	1	1024400	356	0.476	0.440	0.000348	0.923	0.463	-0.155		
-0.05 - 0.05	3	1126293	454	0.524	0.560	0.000403	1.070	0.537	-0.145		
0.05-43.7	43	1	0	0.000	0.000	0.000000	0.000	0.000	0.000		
TOTAL		2150694	810				1.993		0.300	0.700	0.211
Distance to stream(in m)											
-250	1	137976	75	0.064	0.093	0.000544	1.443	0.273	-0.154		
500	2	130169	54	0.061	0.067	0.000415	1.102	0.208	-0.142		
750	3	126049	45	0.059	0.056	0.000357	0.948	0.179	-0.134		
1000	4	125443	39	0.058	0.048	0.000311	0.826	0.156	-0.126		
>3000	5	1631179	597	0.758	0.737	0.000366	0.972	0.184	-0.135		
TOTAL		2150816	810				5.290		0.691	0.309	0.093
TWI											
-2.14 - 5.36	1	857299	508	0.400	0.629	0.000593	1.572	0.504	-0.150		
5.36-6.96	2	764390	235	0.357	0.291	0.000307	0.816	0.262	-0.152		
6.96-9.34	3	348557	52	0.163	0.064	0.000149	0.396	0.127	-0.114		
9.34-13	4	130468	10	0.061	0.012	0.000077	0.203	0.065	-0.077		
13-23.7	5	40172	2	0.019	0.002	0.000050	0.132	0.042	-0.058		
TOTAL		2140886	807				3.119		0.552	0.448	0.135
Elevation (in m)											
-276 - 493	1	377656	12	0.176	0.015	0.000032	0.084	0.010	-0.021		
493-717	2	175695	42	0.082	0.052	0.000239	0.635	0.079	-0.087		
717-915	3	281750	101	0.131	0.125	0.000358	0.952	0.118	-0.110		
915-1095	4	366162	163	0.170	0.201	0.000445	1.182	0.147	-0.122		
1095-1276	5	350282	186	0.163	0.230	0.000531	1.410	0.175	-0.132		

1276-1470	6	302770	139	0.141	0.172	0.000459	1.219	0.151	-0.124		
1470-1708	7	201440	142	0.094	0.175	0.000705	1.872	0.232	-0.147		
1708-2259	8	94808	25	0.044	0.031	0.000264	0.700	0.087	-0.092		
TOTAL		2150563	810				8.053		0.836	0.164	0.050
Lithology											
undivided Precambrian rocks	1	619067	320	0.291	0.395	0.000517	1.356	0.142	-0.120		
Neogene sedimentary rock	2	502911	49	0.236	0.060	0.000097	0.256	0.027	-0.042		
Neogene sedimentary rock	3	67033	9	0.032	0.011	0.000134	0.352	0.037	-0.053		
undivided Precambrian rocks	4	296289	84	0.139	0.104	0.000284	0.744	0.078	-0.086		
Neogene sedimentary rock	5	309429	114	0.145	0.141	0.000368	0.966	0.101	-0.101		
undivided Precambrian rocks	7	169239	60	0.080	0.074	0.000355	0.930	0.097	-0.098		
Paleogene sedimentary rock	8	113902	144	0.054	0.178	0.001264	3.316	0.347	-0.159		
Mesozoic and Paleozoic intrusive and metamorphic rocks	9	49467	31	0.023	0.038	0.000627	1.644	0.172	-0.131		
TOTAL		2127337	811				9.564		0.791	0.209	0.063

CHAPTER-9

WEIGHT OF EVIDENCE

9.1 Introduction:

Weight of Evidence (WoE) is a Bayesian statistical technique that quantifies the influence of conditioning factors on landslide occurrence. For each class of a factor (e.g., a specific slope range), WoE computes two weights:

Positive weight (W^+) measures how much more likely a landslide is in that class compared to the study area overall. Negative weight (W^-) measures how much less likely a landslide is in that class. The difference between positive and negative weights ($W^+ - W^-$) indicates the factor's contribution to susceptibility. In GIS-based mapping, these weights are applied to spatial layers to produce a landslide susceptibility index, effectively highlighting high-risk zones.

9.2 Formula:

It calculates the relationship between landslide occurrences and various conditioning factor classes using statistical weights. It assigns a positive weight (W^+) for areas where landslides are present and a negative weight (W^-) for areas without landslides. Equation 9.1 and 9.2 gives positive weight and negative weight formulas as given below.

$$W_i^+ = \log_e \left[\frac{P(L|S_i)}{P(L)} \right] \quad 9.1$$

$$W_i^- = \log_e \left[\frac{P(-L|S_i)}{P(L)} \right] \quad 9.2$$

The contrast weight (C), which indicates the overall influence of a factor class, is obtained by subtracting the negative weight from the positive weight. A higher contrast value suggests a stronger association with landslide occurrence. Equation 9.3 illustrates the expression for contrast weight.

$$C = W_i^+ + W_i^- \quad 9.3$$

9.3 Outcome:

Weight of Evidence (WoE) method in this study provided a clear and quantifiable understanding of how each conditioning factor contributes to landslide susceptibility. By assigning positive and negative weights to various classes of factors such as slope, lithology, and elevation, the method highlighted areas with higher probabilities of landslide occurrence. The contrast values derived from these weights allowed for the identification of strong correlations between certain terrain features and past landslide events. The resulting susceptibility map effectively categorized the study area into zones of varying risk levels.

9.4 Application:

The Weight of Evidence (WoE) method is a widely applied statistical approach in landslide susceptibility mapping, as it effectively evaluates the relationship between past landslide events and various conditioning factors. Using a Bayesian framework, WoE assigns weights to different classes within each factor—such as slope, lithology, or elevation—based on the presence or absence of landslides. These weights indicate the influence of each class on landslide occurrence. When combined in a GIS environment, these weighted layers help generate detailed susceptibility maps that highlight areas with different risk levels. WoE is valued for its simplicity, clarity, and ability to handle multiple spatial variables, making it a practical tool for landslide hazard analysis and risk planning.

9.5 Advantages:

The Weight of Evidence (WoE) method offers several advantages in landslide susceptibility mapping. It is a straightforward, data-driven approach that relies on statistical relationships between landslide occurrences and conditioning factors, reducing subjectivity in the analysis. WoE allows for easy interpretation of results through positive

and negative weights, which clearly indicate how each factor class contributes to or resists landslides. It performs well in GIS environments, making it efficient for handling large spatial datasets. Additionally, WoE can incorporate multiple variables without complex calculations, making it suitable for regional-scale studies. Its ability to produce reliable susceptibility maps with minimal data makes it a practical and widely used method in landslide risk assessment.

9.6 Data table:

Table 9.1 WEIGHT OF EVIDENCE CALCULATION

LCF	**Total area of Solan**	**2370336**	**Landslide point area**	**761400**	**P(L)**	**0.3212**	**P(-L)**	**0.679**	
Data Layer	**Classes**	**Landslide pixels area**	**Area pixels**	**$P(S_i)$**	**$P(L/S_i)$**	**$P(-L/S_i)$**	**W+**	**W-**	**Weight of contrast**
SLOPE (in degrees)									
0-10	1	10800	484382	0.242	0.022	0.978	-2.668	0.365	-3.033
10'-20	2	154800	597620	0.299	0.259	0.741	-0.215	0.088	-0.303
20-30	3	307800	582647	0.291	0.528	0.472	0.497	-0.364	0.861
30-40	4	207900	271185	0.136	0.767	0.233	0.870	-1.068	1.938
40-50	5	42300	54787	0.027	0.772	0.228	0.877	-1.091	1.968
50-60	6	900	6765	0.003	0.133	0.867	-0.881	0.245	-1.126
60-78	7	900	1627	0.001	0.553	0.447	0.544	-0.418	0.962
Total		**725400**	**1999013**						
ASPECT									
-1 (Flat)	1	1800	11282	0.005	0.160	0.840	-0.700	0.214	-0.913
0-22.5 (North)	2	36000	116611	0.054	0.309	0.691	-0.040	0.018	-0.058
22.5-67.5 (North-east)	3	96300	261477	0.122	0.368	0.632	0.137	-0.072	0.209
67.5-112.5 (East)	4	78300	246419	0.115	0.318	0.682	-0.011	0.005	-0.016
112.5-157.5 (South-east)	5	69300	218320	0.102	0.317	0.683	-0.012	0.006	-0.017
157.5-202.5 (South)	6	91800	279443	0.131	0.329	0.671	0.022	-0.011	0.033
202.5-247.5 (South-west)	7	141300	339281	0.158	0.416	0.584	0.260	-0.151	0.411

247.5-292.5 (West)	8	109800	310660	0.145	0.353	0.647	0.096	-0.049	0.144
292.5-337.5 (North-west)	9	70200	246277	0.115	0.285	0.715	-0.119	0.052	-0.171
337.5-360 (North)	10	31500	111116	0.052	0.283	0.717	-0.125	0.054	-0.179
Total		**726300**	**2140886**						
CURVATURE									
(-33.2- -0.05)	1	320400	1024400	0.476	0.313	0.687	-0.027	0.012	-0.039
(-0.05-0.05)	2	29700	125635	0.058	0.236	0.764	-0.307	0.118	-0.424
(0.05-43.7)	3	378900	1000659	0.465	0.379	0.621	0.164	-0.088	0.253
Total		**729000**	**2150694**						
ROUGHNESS									
0-15	1	12600	561146	0.261	0.022	0.978	-2.661	0.365	-3.025
15-30	2	198000	757619	0.352	0.261	0.739	-0.206	0.085	-0.291
30-45	3	308700	531533	0.247	0.581	0.419	0.592	-0.482	1.074
45-60	4	151200	206615	0.096	0.732	0.268	0.823	-0.929	1.752
60-75	5	50400	78406	0.036	0.643	0.357	0.694	-0.642	1.336
75-272	6	9000	15503	0.007	0.581	0.419	0.592	-0.481	1.073
Total		**729900**	**2150822**						
HILLSHADE									
0-75	1	55800	77860	0.036	0.717	0.283	0.802	-0.874	1.676
75-116	2	127800	213161	0.100	0.600	0.400	0.624	-0.528	1.152
116-148	3	117000	326983	0.153	0.358	0.642	0.108	-0.055	0.163
148-176	4	108000	457823	0.214	0.236	0.764	-0.309	0.118	-0.427
176-206	5	141300	647608	0.303	0.218	0.782	-0.387	0.141	-0.528
206-254	6	172800	413482	0.193	0.418	0.582	0.263	-0.154	0.417
Total		**722700**	**2136917**						
ELEVATION									
293-493	1	10800	377656	0.176	0.029	0.971	-2.419	0.358	-2.777
493-717	2	37800	175695	0.082	0.215	0.785	-0.401	0.145	-0.546
717-915	3	90900	281750	0.131	0.323	0.677	0.004	-0.002	0.006
915-1095	4	146700	366162	0.170	0.401	0.599	0.221	-0.124	0.345
1095-1276	5	167400	350282	0.163	0.478	0.522	0.397	-0.262	0.660
1276-1470	6	125100	302770	0.141	0.413	0.587	0.252	-0.146	0.397
1470-1708	7	127800	201440	0.094	0.634	0.366	0.681	-0.619	1.299
1708-2259	8	22500	94808	0.044	0.237	0.763	-0.303	0.117	-0.419
Total		**729000**	**2150563**						
DISTANCE FROM STREAM (in m)									

250	1	67500	137976	0.064	0.489	0.511	0.421	-0.284	0.705
500	2	48600	130169	0.061	0.373	0.627	0.150	-0.080	0.230
750	3	40500	126049	0.059	0.321	0.679	0.000	0.000	0.000
1000	4	35100	125443	0.058	0.280	0.720	-0.138	0.059	-0.197
>3000	5	537300	1631179	0.758	0.329	0.671	0.025	-0.012	0.037
Total		**729000**	**2150816**						
LITHOLOGY									
pC	1	288000	599067	0.282	0.481	0.519	0.403	-0.268	0.671
N	2	44100	452911	0.213	0.097	0.903	-1.194	0.285	-1.479
N	3	8100	67033	0.032	0.121	0.879	-0.978	0.259	-1.236
pC	4	75600	296289	0.139	0.255	0.745	-0.230	0.093	-0.323
N	5	102600	309429	0.145	0.332	0.668	0.032	-0.015	0.047
pC	7	54000	169239	0.080	0.319	0.681	-0.007	0.003	-0.010
Pg	8	129600	183902	0.086	0.705	0.295	0.786	-0.832	1.618
MzPz	9	27900	49467	0.023	0.564	0.436	0.563	-0.443	1.006
Total		**729900**	**2127337**						
TWI									
2.14-4.3	1	339300	568068	0.265	0.597	0.403	0.620	-0.522	1.142
4.93-6.12	2	248400	719519	0.336	0.345	0.655	0.072	-0.036	0.108
6.12-7.47	3	100800	464101	0.217	0.217	0.783	-0.391	0.143	-0.534
7.47-9.25	4	27000	213126	0.100	0.127	0.873	-0.930	0.252	-1.182
9.25-11.6	5	9000	103064	0.048	0.087	0.913	-1.302	0.296	-1.599
11.6-14.8	6	900	54815	0.026	0.016	0.984	-2.974	0.371	-3.345
14.8-23.7	7	900	18189	0.008	0.049	0.951	-1.871	0.337	-2.207
Total		**726300**	**2140882**						

CHAPTER-10

INFORMATION VALUE

10.1 Introduction:

The Information Value (IV) method is a bivariate statistical technique used in landslide susceptibility mapping to evaluate the link between landslide events and conditioning factors. It assigns weights to each factor class based on landslide frequency, indicating their contribution to landslide risk. Simple, interpretable, and effective, IV helps identify key influencing factors and, when used with GIS, supports the creation of accurate susceptibility maps for hazard planning.

10.2 Formula:

The Information Value (IV) method calculates the contribution of each class of a conditioning factor to landslide occurrence using a logarithmic formula and ratio of conditional probability and prior probability as per equation 10.1 and 10.2.

$$P_{conditional} = \frac{N_{Landslide\ pixels}}{N_{Class\ pixels}} \quad 10.1$$

$$P_{Prior} = \frac{N_{Total\ landslide\ pixels}}{N_{Total\ class\ pixels}} \quad 10.2$$

Using 10.1 and 10.2, we can calculate the information value of each class as given below in equation 10.3.

$$IV = \log_e \frac{P_{conditional}}{P_{prior}} \quad 10.3$$

10.3 Outcome:

The use of the Information Value (IV) method in landslide susceptibility mapping provided the most accurate results among the models applied in this study. By assigning statistical weights based on the frequency of landslides within different classes of conditioning factors, the IV method effectively highlighted the factors most strongly associated with slope failures. The resulting susceptibility map clearly delineated areas of low to very high landslide risk, offering valuable insights for hazard assessment and land-use planning

10.4 Application:

The Information Value (IV) method is applied in landslide susceptibility mapping to assess the influence of various conditioning factors by assigning weights based on landslide frequency. It helps identify which factors contribute most to landslide occurrences and supports the classification of areas into different risk zones. IV is particularly useful for generating data-driven susceptibility maps in a GIS environment, aiding in hazard assessment, land-use planning, and targeted risk mitigation. It can also be used alongside other models for comparative analysis of predictive performance.

10.5 Advantages:

The Information Value (IV) method offers several advantages in landslide susceptibility mapping. It is simple to apply and easy to interpret, making it suitable for a wide range of users. IV effectively quantifies the influence of each conditioning factor based on landslide frequency, allowing for objective and data-driven analysis. It performs well with large datasets and integrates easily with GIS tools for spatial mapping. Additionally, IV helps identify the most significant contributing factors, improving the accuracy of susceptibility maps and supporting informed decision-making in hazard

assessment and land-use planning.

11.0 Data Table:

Table 10.1 INFORMATION VALUE CALCULATION

		Total area of Solan	**2370336**		**Landslide area pixels**	**761400**	
Data Layer	**Classes**	**Area pixels**	**Landslide pixels area**	**Conditional probability**	**Prior probabilty**	**C_p/P_p**	**INFORMATION VALUE**
SLOPE (in degrees)							
0-10	1	484382	10800	0.022	0.363	0.061	-1.212
10'-20	2	597620	154800	0.259	0.363	0.714	-0.146
20-30	3	582647	307800	0.528	0.363	1.456	0.163
30-40	4	271185	207900	0.767	0.363	2.113	0.325
40-50	5	54787	42300	0.772	0.363	2.128	0.328
50-60	6	6765	900	0.133	0.363	0.367	-0.436
60-78	7	1627	900	0.553	0.363	1.524	0.183
Total		**1999013**	**725400**				
ASPECT							
-1 (Flat)	1	11282	1800	0.160	0.339	0.470	-0.328
0-22.5 (North)	2	116611	36000	0.309	0.339	0.910	-0.041
22.5-67.5 (North-east)	3	261477	96300	0.368	0.339	1.086	0.036
67.5-112.5 (East)	4	246419	78300	0.318	0.339	0.937	-0.028
112.5-157.5 (South-east)	5	218320	69300	0.317	0.339	0.936	-0.029
157.5-202.5 (South)	6	279443	91800	0.329	0.339	0.968	-0.014
202.5-247.5 (South-west)	7	339281	141300	0.416	0.339	1.228	0.089
247.5-292.5 (West)	8	310660	109800	0.353	0.339	1.042	0.018
292.5-337.5 (North-west)	9	246277	70200	0.285	0.339	0.840	-0.076
337.5-360 (North)	10	111116	31500	0.283	0.339	0.836	-0.078
Total		**2140886**	**726300**				
CURVATURE							
(-33.2- -0.05) Concave	1	1024400	320400	0.313	0.339	0.923	-0.035

(-0.05-0.05)	2	125635	29700	0.236	0.339	0.697	-0.157
(0.05-43.7)	3	1000659	378900	0.379	0.339	1.117	0.048
Total		**2150694**	**729000**				
ROUGHNESS							
0-15	1	561146	12600	0.022	0.339	0.066	-1.179
15-30	2	757619	198000	0.261	0.339	0.770	-0.113
30-45	3	531533	308700	0.581	0.339	1.711	0.233
45-60	4	206615	151200	0.732	0.339	2.156	0.334
60-75	5	78406	50400	0.643	0.339	1.894	0.277
75-272	6	15503	9000	0.581	0.339	1.711	0.233
Total		**2150822**	**729900**				
HILLSHADE							
0-75	1	77860	55800	0.717	0.338	2.119	0.326
75-116	2	213161	127800	0.600	0.338	1.773	0.249
116-148	3	326983	117000	0.358	0.338	1.058	0.024
148-176	4	457823	108000	0.236	0.338	0.698	-0.156
176-206	5	647608	141300	0.218	0.338	0.645	-0.190
206-254	6	413482	172800	0.418	0.338	1.236	0.092
Total		**2136917**	**722700**				
ELEVATION							
293-493	1	377656	10800	0.029	0.339	0.084	-1.074
493-717	2	175695	37800	0.215	0.339	0.635	-0.197
717-915	3	281750	90900	0.323	0.339	0.952	-0.021
915-1095	4	366162	146700	0.401	0.339	1.182	0.073
1095-1276	5	350282	167400	0.478	0.339	1.410	0.149
1276-1470	6	302770	125100	0.413	0.339	1.219	0.086
1470-1708	7	201440	127800	0.634	0.339	1.872	0.272
1708-2259	8	94808	22500	0.237	0.339	0.700	-0.155
Total		**2150563**	**729000**				
DISTANCE FROM STREAM (in m)							
250	1	137976	67500	0.489	0.339	1.443	0.159
500	2	130169	48600	0.373	0.339	1.102	0.042
750	3	126049	40500	0.321	0.339	0.948	-0.023
1000	4	125443	35100	0.280	0.339	0.826	-0.083
>3000	5	1631179	537300	0.329	0.339	0.972	-0.012
Total		**2150816**	**729000**				
LITHOLOGY							
pC	1	599067	288000	0.481	0.343	1.401	0.146
N	2	452911	44100	0.097	0.343	0.284	-0.547
N	3	67033	8100	0.121	0.343	0.352	-0.453

pC	4	296289	75600	0.255	0.343	0.744	-0.129
N	5	309429	102600	0.332	0.343	0.966	-0.015
pC	7	169239	54000	0.319	0.343	0.930	-0.032
Pg	8	183902	129600	0.705	0.343	2.054	0.313
MzPz	9	49467	27900	0.564	0.343	1.644	0.216
Total		**2127337**	**729900**				
TWI							
2.14-4.3	1	568068	339300	0.597	0.339	1.761	0.246
4.93-6.12	2	719519	248400	0.345	0.339	1.018	0.008
6.12-7.47	3	464101	100800	0.217	0.339	0.640	-0.194
7.47-9.25	4	213126	27000	0.127	0.339	0.373	-0.428
9.25-11.6	5	103064	9000	0.087	0.339	0.257	-0.589
11.6-14.8	6	54815	900	0.016	0.339	0.048	-1.315
14.8-23.7	7	18189	900	0.049	0.339	0.146	-0.836
Total		**2140882**	**726300**				

CHAPTER 11

RESULTS

11.1 Discussion:

Landslide Susceptibility Maps were created using three different methods: Shannon Entropy (SE), Information Value (IV), and Weight of Evidence (WoE). These models assist in detecting areas at risk of landslides by evaluating environmental factors like slope, elevation, aspect, and lithology.

Each method uses a distinct approach to assign weights to the contributing factors, leading to varying classifications of landslide susceptibility.

Shannon Entropy (SE): It quantifies the uncertainty associated with each factor classes to determine its influence on landslide occurrence.

Weight of Evidence (WoE): a Bayesian approach statistical technique which calculates positive and negative weights based on the presence or absence of landslides and relating them to different factor classes.

Information Value (IV): It is a bivariate statistical method which assigns weights based on the frequency of landslide events within each class of a conditioning factor.

These models facilitated a comparative evaluation of landslide-prone areas by highlighting how each method interprets the influence of environmental factors, thereby offering insights into the strengths and differences in their susceptibility classifications.

Based on AUC-ROC values, Information value (IV) (AUC= 0.737) showed the highest predictive accuracy, followed by Shannon Entropy (SE) (AUC= 0.719) and Weight of Evidence WoE (AUC= 0.632), highlighting the varying effectiveness of each method in classifying risk areas. Both models showed high predictive performance, emphasizing the reliability and effectiveness of statistical, data-driven methods in landslide susceptibility assessment. However, WoE model provides lower AUC value

indicating limitation in weight assignment, data quality and broad classification of LCF classes. This comparison provides insight into model performance and supports the selection of appropriate approaches for future susceptibility mapping.

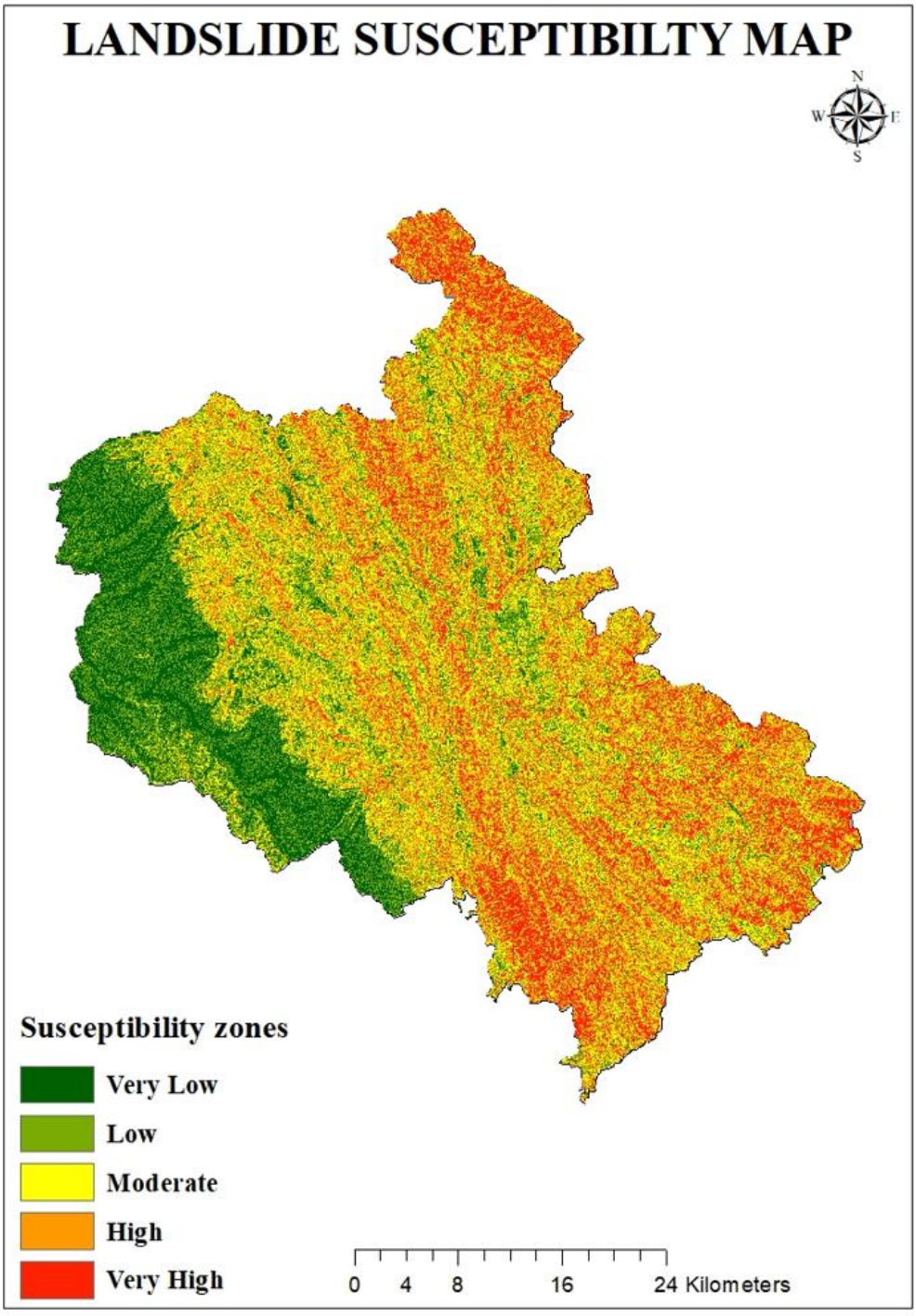

Figure 11.1 Landslide susceptibility map using Shannon Entropy

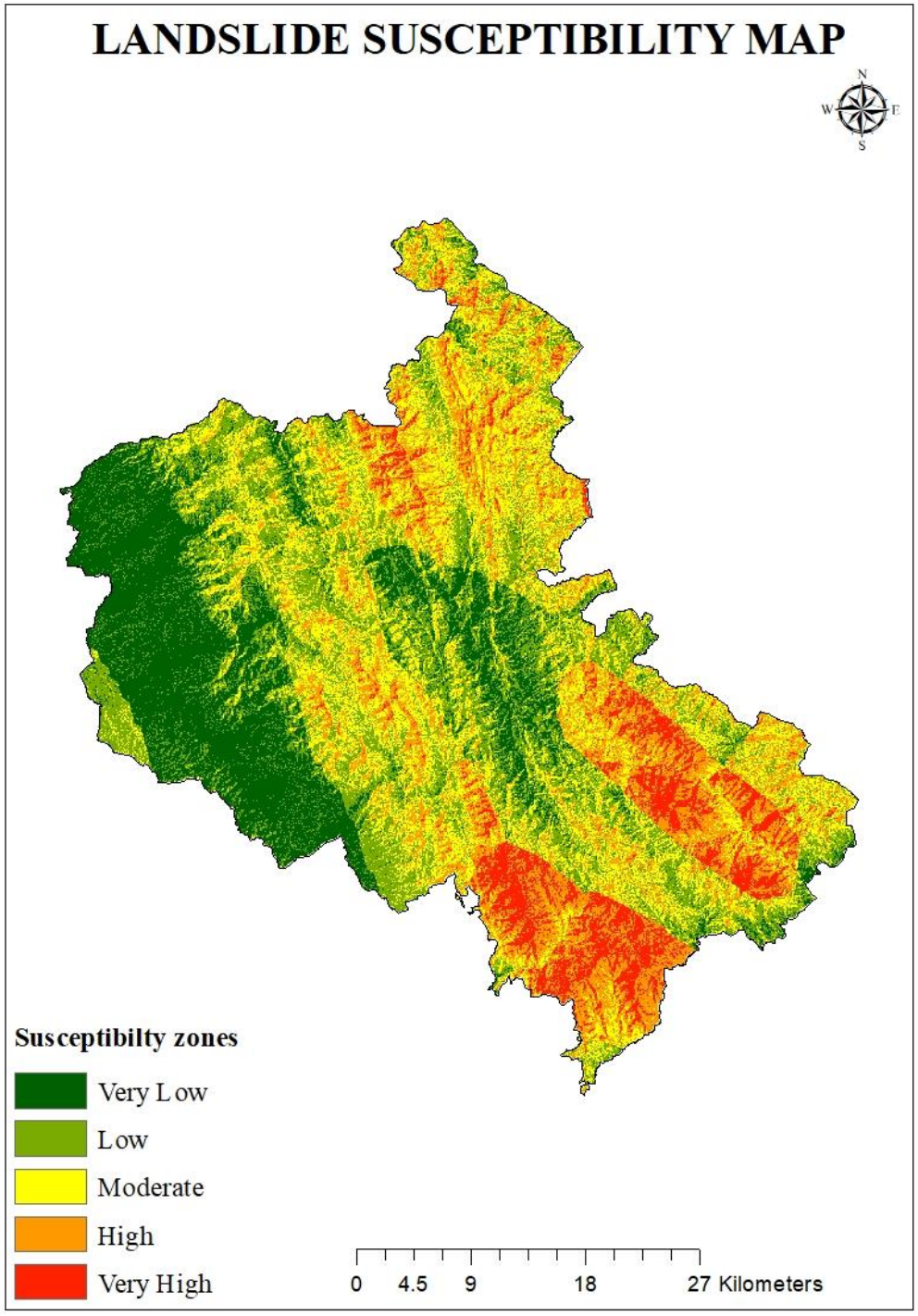

Figure 11.2 Landslide susceptibility map using Weight of Evidence

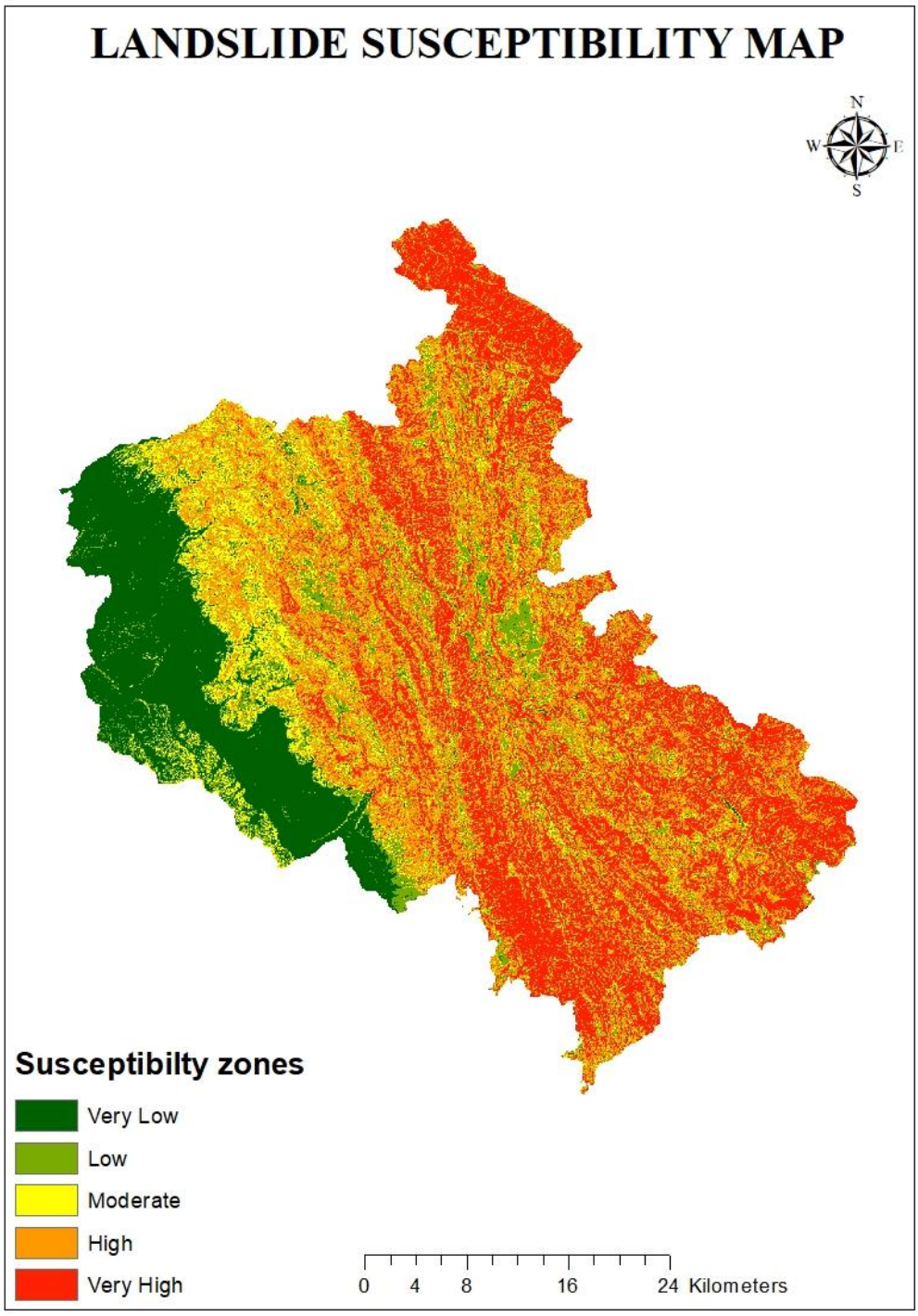

Figure 11.3 Landslide susceptibility map using Information Value

11.2 Validation:

Validation plays a key role in evaluating the accuracy and reliability of a predictive model. It confirms that the model not only fits the training data well but also performs effectively on new, unseen data. In landslide susceptibility mapping and similar applications, validation helps assess how accurately the model distinguishes between susceptible and non-susceptible areas. Techniques like k-fold cross-validation, hold-out validation, AUC-ROC and various statistical metrics are commonly used to measure model performance.

During validation, success rate curve is one of the most important things because it helps us understand how accurately the model identifies landslide-prone areas based on past data. If most landslides fall within the zones the model marks as high-risk, it means the model is performing well. A steep curve indicates that the model correctly identifies high-susceptibility zones early in the ranking. This helps researchers trust that the model is reliability and suitability.

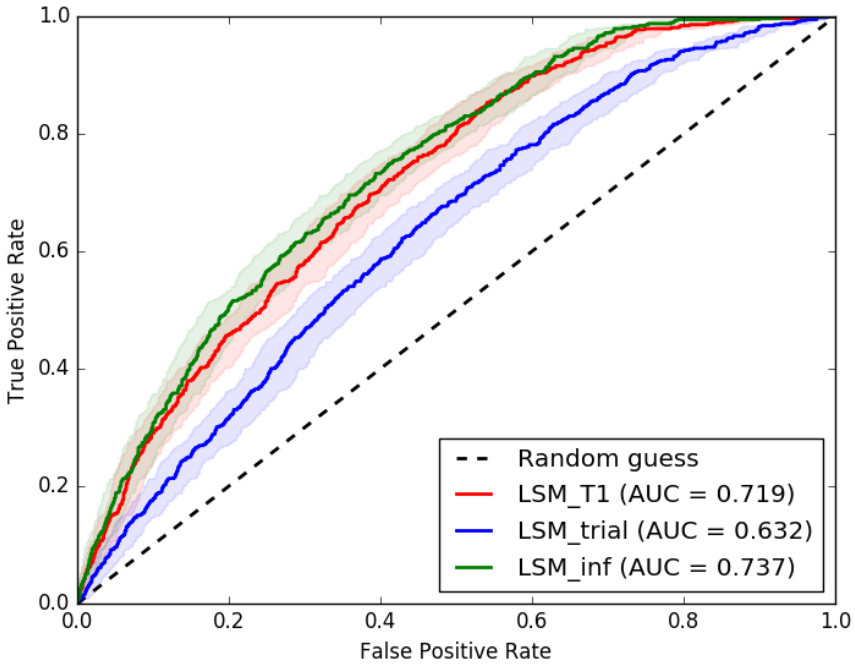

Figure 11.4 Success rate curve

Similarly, the Prediction Rate Curve assesses how well the model can predict landslide occurrences using an independent testing dataset. It evaluates the model's ability to generalize beyond the data it was trained on. A high prediction rate suggests that the model performs reliably on unseen data, indicating strong generalization and making it suitable for real-world applications in hazard assessment and planning.

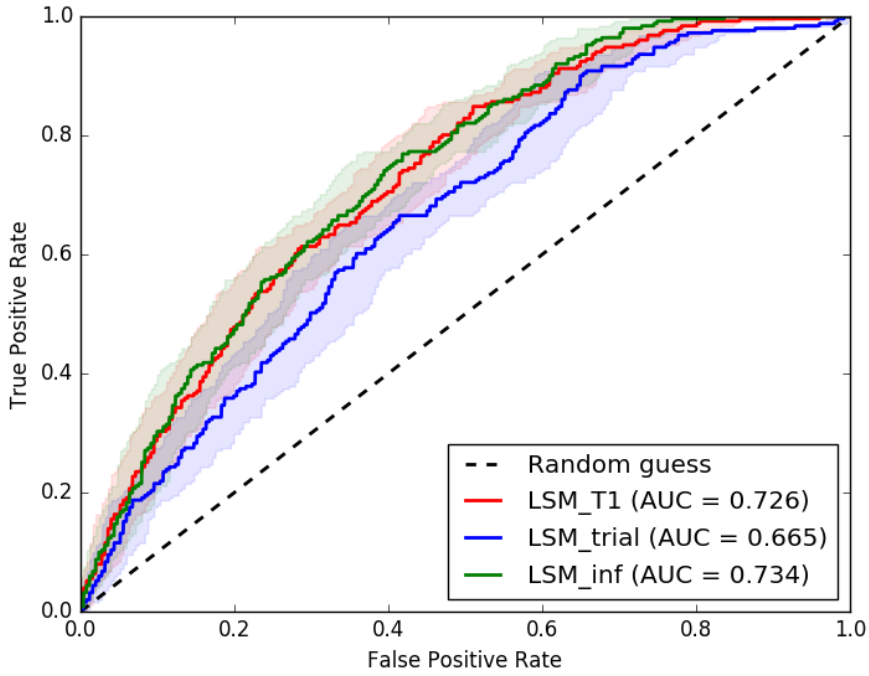

Figure 11.5 Prediction rate curve

In evaluating the performance of a landslide susceptibility model using AUC-ROC, the classification outcomes are essential. True Positives (TP) represent areas where landslides were correctly predicted, while True Negatives (TN) are areas correctly identified as safe. False Positives (FP) occur when the model wrongly classifies a safe area as landslide-prone, and False Negatives (FN) are instances where actual landslides were missed by the model. These classifications directly affect key performance metrics. Accuracy measures the overall correctness of the model, combining both correct predictions (TP and TN). Sensitivity (or recall) reflects the model's ability to correctly identify actual landslide areas, relying on TP and FN. Specificity evaluates how well the model identifies non-landslide areas, based on TN and FP. Together, these values shape the ROC curve, and

the Area Under the Curve (AUC) summarizes the model's reliability. A higher AUC indicates that the model consistently distinguishes between landslide and non-landslide areas, making it more dependable for real-world application.

CHAPTER-12

CONCLUSION AND FUTURE FOCUS

12.1 Conclusion:

This study focused on landslide susceptibility mapping in the Solan district of Himachal Pradesh using three statistical models: Shannon Entropy (SE), Information Value (IV), and Weight of Evidence (WoE). Landslide susceptibility maps were generated for each model, and their performance was evaluated using both training (70%) and testing (30%) datasets. The generated susceptibility maps were validated using Area Under the Curve (AUC) values for the training data were achieved from Information Value (IV) (AUC=0.737), followed closely by Shannon Entropy (SE) (AUC=0.719), and Weight of Evidence (WoE) had (AUC=0.632). These results indicate that both SE and IV demonstrated strong predictive capabilities, while WoE showed limitations, likely due to its assumption of factor independence during weight assignment.

Success Rate and Prediction Rate curves were also developed to assess how well each model fit the training data and how accurately it predicted new landslide events. The findings clearly suggest that SE and IV outperform WoE in identifying landslide-prone zones. As a result, these two models can be considered more reliable for practical applications such as disaster risk reduction, land-use planning, and the development of future infrastructure in landslide-prone regions like Solan.

12.2 Future focus:

The comparative study between Information Value (IV), Shannon Entropy (SE), and Weight of Evidence (WoE) has been efficiently done, showcasing that the models IV and SE perform better than WoE in landslide susceptibility mapping. Future research can explore the integration of machine learning techniques such as Decision Tree, Random Forest, Support Vector Machines, and Deep Learning to improve prediction accuracy. Incorporating additional environmental variables like soil moisture, vegetation indices, and rainfall variability can further enhance model precision.

Technical advancements may also include the development of hybrid models that combine statistical, analytical, and machine learning methods for more robust susceptibility mapping. Conducting temporal analyses can reveal how landslide patterns evolve over time, while on-ground field validation will help ensure the models reflect real-world conditions. These enhancements will contribute to the creation of more adaptive, accurate, and data-driven models, ultimately strengthening disaster preparedness and landslide risk mitigation in vulnerable areas.

REFERENCES

- A., C., Valvo, M. S., & Reali, C. (1982). Analysis of landslide form and incidence by statistical techniques, Southern Italy. *CATENA, 9*(1), 35-62.
- Agung, P. M., Hasan, M. R., Susilo, A., Ahmad, M. A., Ahmad, M. B., Abdurrahman, U., . . . Suryo, E. A. (2023). Compilation of Parameter Control for Mapping the Potential Landslide Areas. *Civil Engineering Journal, 9*(4), 974-989.
- Aksoy, H. (2023). Determination of landslide susceptibility with Analytic Hierarchy Process (AHP) and the role of forest ecosystem services on landslide susceptibility. *Environmental Monitoring and Assessment*, 1525.
- Cárdenas, N. Y., & Mera , E. E. (2016). Landslide susceptibility analysis using remote sensing and GIS in the western Ecuadorian Andes. *Natural Hazards, 81*(3), 1829-1859.
- Chen, W., & Zhang, S. (2021). GIS-based comparative study of Bayes network, Hoeffding tree and logistic model tree for landslide susceptibility modeling. *Catena*.
- Chen, W., Zhang, S., Li, R., & Shahabi, H. (2018). Performance evaluation of the GIS-based data mining techniques of best-first decision tree, random forest, and naïve Bayes tree for landslide susceptibility modeling. *Science of The Total Environment, 644*, 1006-1018.
- Duman, T., Can, T., Gokceoglu, C., Nefeslioglu, H., & Sonmez, H. (2006). Application of logistic regression for landslide susceptibility zoning of Cekmece Area, Istanbul, Turkey. *Environmental Geology, 51*(2), 241-256.
- Fayez, L., Binh, T. P., Solanki, H., Pazhman, D., Dholakia, M., Khalid, M., & Prakash, I. (2018). Application of frequency ratio model for the development of landslide susceptibility mapping at part of Uttarakhand State, India. *International Journal of Applied Engineering Research*, 6846-6854.
- Hong, H., Miao, Y., Liu, J., & Zhu, A.-X. (2019). Exploring the effects of the

design and quantity of absence data on the performance of random forest-based landslide susceptibility mapping. *CATENA, 176*, 45-64.

- Hong, H., Naghibi, S. A., Pourghasemi, H. R., & Pradhan, B. (2016). GIS-based landslide spatial modeling in Ganzhou City, China. *Arabian Journal of Geosciences*, 1-26.
- Jallayu, P. T., Sharma, A., & Singh, K. (2024). Vulnerability of highways to landslide using landslide susceptibility zonation in GIS: Mandi district, India. *Innovative Infrastructure Solutions*, 354.
- Jierui, L., Wen , H., Lingke, Q., Wen, Z., & Baofeng , D. (2024). Landslide Susceptibility Assessment Based on Machine Learning Techniques. In R. Sarkar, S. Saha, B. R. Adhikari, & R. Shaw, *Geomorphic Risk Reduction Using Geospatial Methods and Tools* (pp. 3-27). Singapore: Springer.
- Kincal, C., & Kayhan, H. (2022). A Combined Method for Preparation of Landslide Susceptibility Map in Izmir. *Applied Sciences*, 9029.
- Lestari, S., & Suratman. (2022). The susceptibility of landslide zone using weight of evidence method in nagari tanjung sani and nagari sungai batang, west sumatera. *IOP Conference Series: Earth and Environmental Science*.
- Miller, S., & Degg, M. (2012). Landslide susceptibility mapping in North-East Wales. *Geomatics, Natural Hazards and Risk*, 139-159.
- Nohani, E., Moharrami, M., Sharafi, S., Khosravi, K., Pradhan, B., Pham, B. T., . . . Melesse, A. M. (2019). Landslide Susceptibility Mapping Using Different GIS-Based Bivariate Models. *Water*, 1402.
- Pattanaik, A., Singh, T. K., & Saxe, M. (2019). Landslide Susceptibility Mapping Using AHP Along Mechuka Valley, Arunachal Pradesh, India. In P. J. Rao, K. N. Rao, & S. Kubo, *Proceedings of International Conference on Remote Sensing for Disaster Management* (pp. 635-651). Springer.
- Peng, L., Sun, Y., Zhan, Z., Shi, W., & Zhang, M. (2023, 12 31). FR-weighted GeoDetector for landslide susceptibility and driving factors analysis. *Geomatics, Natural Hazards and Risk, 14*(1).

- Poudyal, C. P., Chang, C., Oh, H.-J., & Lee, S. (2010, 9 4). Landslide susceptibility maps comparing frequency ratio and artificial neural networks: a case study from the Nepal Himalaya. *Environmental Earth Sciences, 61*(5), 1049-1064.
- Pourghasemi, H. R., Jirandeh, A. G., Pradhan, B., Chong, X., & Candan, G. (2013). Landslide susceptibility mapping using support vector machine and GIS at the Golestan Province, Iran. *Journal of Earth System Science, 122*, 349-369.
- Pourghasemi, H. R., Mohammady, M., & Pradhan, B. (2012). Landslide susceptibility mapping using index of entropy and conditional probability models in GIS: Safarood Basin, Iran. *CATENA, 97*, 71-84.
- Pourghasemi, H., Moradi, H., & Aghda, S. F. (2013). Landslide susceptibility mapping by binary logistic regression, analytical hierarchy process, and statistical index models and assessment of their performances. *Natural hazards*, 749-779.
- Saha, A., Roy, B., Saha, S., Chaudhary, A., & Sarkar, R. (2024). An Advanced Hybrid Machine Learning Technique for Assessing the Susceptibility to Landslides in the Upper Meenachil River Basin of Kerala, India. In R. Sarkar, S. Saha, B. R. Adhikari, & R. Shaw, *Geomorphic Risk Reduction Using Geospatial Methods and Tools* (pp. 61-77). Singapore: Springer Nature Singapore.
- Saha, S., Saha, A., Roy, B., Chaudhary, A., & Sarkar, R. (2024). Artificial Neural Network Ensemble with General Linear Model for Modeling the Landslide Susceptibility in Mirik Region of West Bengal, India. In *Geomorphic Risk Reduction Using Geospatial Methods and Tools* (pp. 41-59). Singapore: Springer Nature Singaore.
- Saha, S., Saha, A., Sarkar, R., Mukherjee, K., Bhardwaj, D., & Kumar, A. (2024). Measuring Landslide Susceptibility in Jakholi Region of Garhwal Himalaya Using Landsat Images and Ensembles of Statistical and Machine Learning Algorithms. In R. Sarkar, S. Saha, B. R. Adhikari, & R. Shaw, *Geomorphic Risk Reduction Using Geospatial Methods and Tools* (pp. 219-249). Singapore: Springer Nature Singapore.
- Sarkar, R., Sujeewon, B. C., & Pawar, A. (2024). Landslide Susceptibility

Mapping Using Satellite Images and GIS-Based Statistical Approaches in Part of Kullu District, Himachal Pradesh, India. In R. Sarkar, S. Saha, B. R. Adhikari, & R. Shaw, *Geomorphic Risk Reduction Using Geospatial Methods and Tools* (pp. 251-287). Singapore: Springer Nature Singapore.

- Singh, P., Sharma, A., Sur, U., & Rai, P. K. (2021). Comparative landslide susceptibility assessment using statistical information value and index of entropy model in Bhanupali-Beri region, Himachal Pradesh, India. *Environment, Development and Sustainability, 23*(4), 5233-5250.
- Taalab, K., Cheng, T., & Zhang, Y. (2018). Mapping landslide susceptibility and types using Random Forest. *Big Earth Data*, 159-178.
- Trinh, T., Luu, B. T., Nguyen, D. H., Le, T. H., Pham, S. V., & VoungThi, N. (2023). A study of non-landslide samples and weights for mapping landslide susceptibility using regression and clustering methods. *Earth Science Informatics, 16*(4), 4009-4034.
- Yang, S., Li , D., Sun, Y., & She, X. (2024). Effect of landslide spatial representation and raster resolution on the landslide susceptibility assessment. *Environmental Earth Sciences, 83*(4), 132.

PUBLICATIONS

1. International Conference on Geological and Environmental Sustainability (ICGES-25)

Sharma, S., Sagar, D. & Sarkar, R. GIS-Based Comparative Analysis of Landslide Susceptibility Using Shannon Entropy, Weight of Evidence, and Information Value: A Case Study of Solan District. International Conference on Geological and Environmental Sustainability (ICGES-25), 03rd-May-2025, Chandigarh, India

SFE
SOCIETY FOR EDUCATION

International Conference on Geological and Environmental Sustainability (ICGES-25)

03rd-May-2025 | Chandigarh, India

Acceptance Letter

Paper ID: SFE_61805

Paper Title: GIS-Based Comparative Analysis of Landslide Susceptibility Using Shannon Entropy, Weight of Evidence, and Information Value: A Case Study of Solan District

Authors Name: Shivakar Sharma, Dhiren Sagar, Raju Sarkar

Dear Author,

With heartiest congratulations I am pleased to inform you that based on the recommendations of the reviewers and the Technical Program Committees, your paper identified above has been accepted for publication and oral presentation by **International Conference on Geological and Environmental Sustainability (ICGES-25)**

This conference received number of submissions from different countries and regions, reviewed by international experts and your paper cleared all the criteria, got accepted for the conference. Your paper will be published in the conference proceeding after the registration.

For registration: https://www.sfe.net.in/conf/registration.php?id=3331560

Herewith, the conference committee sincerely invites you to come to present your paper at our conference.

Sincerely,

Dr. James Crusoe
President
Society for Education (SFE)

+91 9677007228 info@sfe.net.in www.sfe.net.in


Google Scholar
CERTIFICATE
OF PRESENTATION
SFE
International Conference on Geological and Environmental Sustainability (ICGES-25)
03rd May 2025 | Chandigarh - India
This is to certify that Shivakar Sharma affiliated with
Delhi Technological University, India has presented a paper titled
GIS-Based Comparative Analysis of Landslide Susceptibility Using Shannon Entropy, Weight of Evidence, and
Information Value: A Case Study of Solan District
at the conference organized by the Society For Education (SFE) held on 03rd May 2025 at Chandigarh - India.
DOI Directory .com Identifying Articles
Dr. James Crusoe
President, SFE
SOCIETY FOR EDUCATION SFE INTERNATIONAL CONFERENCE
Shraddha Srinath
Convener
Crossref

2. International Conference on Interdisciplinary Academic Research and Innovation (IARI-25)

Sharma, S., Sarkar, R. A Shannon Entropy-Based GIS Approach for Landslide Susceptibility Mapping in Solan District, Himachal Pradesh. International Conference on Interdisciplinary Academic Research and Innovation (IARI-25), 18th-May-2025, Agra, India

SOCIETY FOR EDUCATION

International Conference on Interdisciplinary Academic Research and Innovation(IARI-25)

18th May 2025 | Agra, India

Acceptance Letter

Paper ID: SFE_19846

Paper Title: A Shannon Entropy-Based GIS Approach for Landslide Susceptibility Mapping in Solan District, Himachal Pradesh

Authors Name: Shivakar Sharma, Raju Sarkar

Dear Author,

With heartiest congratulations I am pleased to inform you that based on the recommendations of the reviewers and the Technical Program Committees, your paper identified above has been accepted for publication and oral presentation by **International Conference on Interdisciplinary Academic Research and Innovation(IARI-25)**

This conference received number of submissions from different countries and regions, reviewed by international experts and your paper cleared all the criteria, got accepted for the conference. Your paper will be published in the conference proceeding after the registration.

For registration: https://www.sfe.net.in/conf/registration.php?id=3337742

Herewith, the conference committee sincerely invites you to come to present your paper at our conference.

Sincerely,

Dr. James Crusoe
President
Society for Education (SFE)

+91 9677007228 info@sfe.net.in www.sfe.net.in


Google Scholar
CERTIFICATE
OF PRESENTATION
SFE
International Conference on Interdisciplinary Academic Research and Innovation (IARI-25)
18th May 2025 | Agra - India
This is to certify that.....Shivakar Sharma.....affiliated with
.....Delhi Technological University, Delhi, India.....has presented a paper titled
A Shannon Entropy-Based GIS Approach for Landslide Susceptibility Mapping in Solan District, Himachal Pradesh
at the conference organized by the Society For Education (SFE) held on 18th May 2025 at Agra - India.
DOI Directory .com Identifying Articles
Dr. James Crusoe
President, SFE
SOCIETY FOR EDUCATION SFE INTERNATIONAL CONFERENCE
Shraddha Srinath
Convener
Crossref